Bioorganic & Medicinal Chemistry Letters 26 (2016) 1485–1489

Contents lists available at ScienceDirect

Bioorganic & Medicinal Chemistry Letters

journal homepage: www.elsevier.com/locate/bmcl

The natural flavone fukugetin as a mixed-type inhibitor for human tissue kallikreins

Jorge A. N. Santos [a,†], Márcia Y. Kondo [b,†], Renato F. Freitas [c], Marcelo H. dos Santos [d], Teodorico C. Ramalho [e], Diego M. Assis [b], Luiz Juliano [b], Maria A. Juliano [b], Luciano Puzer [f,*]

[a] Instituto Federal de Ciência, Tecnologia e Educação do Sul de Minas Gerais, Campus Inconfidentes, MG, Brazil
[b] Departamento de Biofísica, Universidade Federal de São Paulo, São Paulo, SP, Brazil
[c] Department of Biology, The Johns Hopkins University, Baltimore, MD, USA
[d] Departamento de química, Universidade Federal de Viçosa, Viçosa, MG, Brazil
[e] Departamento de química, Universidade Federal de Lavras, Lavras, MG, Brazil
[f] Centro de Ciências Naturais e Humanas, Bloco Delta, Sala 210, Universidade Federal do ABC, Rua Arcturus 3, São Bernardo do Campo, SP 09606-070, Brazil

ARTICLE INFO

Article history:
Received 13 July 2015
Revised 12 January 2016
Accepted 14 January 2016
Available online 23 January 2016

Keywords:
Enzyme
Serine protease
Kallikrein
Inhibitor
Flavone
Molecular docking
Molecular dynamic simulation

ABSTRACT

The human tissue kallikreins (KLK1–KLK15) comprise a family of 15 serine peptidases detected in almost every tissue of the human body and that actively participate in many physiological and pathological events. Some kallikreins are involved in diseases for which no effective therapy is available, as for example, epithelial disorders, bacterial infections and in certain cancers metastatic processes. In recent years our group have made efforts to find inhibitors for all kallikreins, based on natural products and synthetic molecules, and all the inhibitors developed by our group presented a competitive mechanism of inhibition. Here we describe fukugetin, a natural product that presents a mixed-type mechanism of inhibition against KLK1 and KLK2. This type of inhibitor is gaining importance today, especially for the development of exosite-type inhibitors, which present potential to selectively inhibit the enzyme activity only against specific substrate.

The family of the tissue kallikrein and kallikrein-related peptidases (KLKs), encoded by the largest contiguous cluster of protease genes in the human genome, consists of 15 homologous, single-chain, secreted serine proteases. They possess at least 30% sequence identity and the mature proteins are approximately of ~25–30 kDa, with similar structural characteristics and trypsin- or chymotrypsin-like specificities.[1,2] KLKs are synthesized as zymogens, secreted and then proteolytically processed to generate the active form. Proteolytic activity of KLKs is also regulated by complex formation with endogenous plasma and tissue inhibitors such as α2-macroglobulin and serpins, and/or inactivation through self-fragmentation.[3] All KLKs have different expression patterns and physiological roles in different tissues with diverse functions and substrates. Based on KLK1–kininogen interaction, the crystal structures of KLKs complexes and the functional data define three distinct regions in the protease domain as important to recognition of substrate and inhibitors; (i) the S1 pocket; (ii) kallikrein loop and S2–S4 pockets; (iii) S1′–2′ pockets.[4]

The expression of KLKs occurs in many organs including skin, pancreas, colon, brain, breast and prostate, where epithelial cells mainly secrete them. Once secreted, KLKs remain in the pericellular space or enter body fluids such as saliva, sweat, milk, seminal plasma and cerebrospinal fluid.[5] The physiological processes in which KLKs are involved include regulation of blood pressure (KLK1-mediated cleavage of kininogenase), extracellular-matrix remodeling (KLK3, 5, 6, 13 and 14) skin desquamation (KLK5, KLK7, and KLK14), neural plasticity (KLK6–8), semen liquefaction (PSA/KLK3- and KLK2-mediated cleavage of semenogelins) among others. KLKs are able to cleave and, consequently, to activate cell surface receptors and other proteases, being part of proteolytic cascades and signal transduction pathways and networks.[6–11]

In addition to the so far described physiological roles of KLKs, their unusual expression and activity have been reported in various pathological conditions such as Alzheimer's disease and in many cancer-related processes, such as cell growth regulation, angiogenesis, invasion, and metastasis, being KLK3/PSA one of the most important biomarkers for prostate cancer.[12–14] Thus,

* Corresponding author. Tel.: +55 11 2320 6238.
E-mail address: luciano.puzer@ufabc.edu.br (L. Puzer).
† Both authors contributed equally to this work.

http://dx.doi.org/10.1016/j.bmcl.2016.01.039
0960-894X/

the search for new KLKs inhibitors is necessary either to elucidate roles of KLKs in many physiological and pathological processes or to be used as potential therapy in many diseases.[7,15] In recent years our group have described different competitive inhibitors for kallikreins, based on natural products and synthetic molecules.[16–18]

Here we describe fukugetin, a natural product that presents a mixed-type mechanism of inhibition against KLK1 and KLK2. This type of inhibitor is gaining importance today, especially for the development of exosite-type inhibitors, which present potential to selectively inhibit the enzyme activity only against specific substrate. In this study, we report the inhibition of KLKs 1, 2, 3, 5, 6 and 7 activities by fukugetin (Table 1), compound isolated from *Garcinia brasiliensis*. Fukugetin is a plant flavonoids compound that consists of a naringenin covalently linked to a luteolin, that is a flavanone-(C-3 → C-8″)-flavone biflavonoid, like others biflavones, presents rigidity of benzopyranone moiety as well as flexibility between phenyl ring and benzopyranone and it was previously shown to be a potent inhibitor of cysteine proteases papain and cruzain with slow-binding and reversibility kinetics.[19]

Fukugetin was extracted and isolated from *G. brasiliensis* fruit as previously described.[16] The fruits were collected at the herbarium of the University of Viçosa (latitude 20° 45′ 14″ south and longitude 42° 52 ′ 55″ west), Minas Gerais, Brazil. Mature kallikreins were expressed and purified from a baculovirus/insect cell line system as previously described.[17] Enzymes concentrations were determined by the method of Bradford.[20] Purity and characterization of the enzymes were confirmed by SDS/PAGE, N-terminal sequencing, and mass spectrometry. Kallikrein proteolytic activity was monitored on the fluorescence resonance energy transfer (FRET) peptides, Abz-KLRSSQ-EDDnp (for KLK1, KLK2, KLK5 and KLK6) and Abz-KLYSSQ-EDDnp (for KLK3 and KLK7) as previously described.[15] To measure the kinetic parameters, all kallikreins (final concentrations ~10 nM) were incubated with fukugetin in increasing concentrations (final concentrations were 1, 2, 6, 8 and 10 μM) in a final volume of 1 ml using as buffer 50 mM Tris, 1 mM EDTA, pH 7.5 at 37 °C. After 10 min of incubation, hydrolytic activity was assayed in a Hitachi F-2500 spectrofluorimeter by the addition of FRET peptides (in five different concentrations 0.25–10 μM). Fluorescence changes were monitored continuously at a λ_{ex} of 320 nm and λ_{em} of 420 nm. Furthermore, the IC_{50} values were determined from plots of percent inhibition versus log inhibitor concentration and calculated by nonlinear regression using the KaleidaGraph program. This software was also used to calculate K_m and V_{max} values by nonlinear regression. Factors α, β and K_i for KLK1 and KLK2 inhibition were calculated using Eqs. 1 and 2, which describe a linear partial competitive inhibition [23], where K_S is the substrate dissociation constant:

$$\text{Slope} = \frac{K_s}{K_i V_{max}}[I] + \frac{K_s}{V_{max}} \quad (1)$$

$$\text{Intercept} = \frac{1}{\alpha K_i V_{max}}[I] + \frac{1}{V_{max}} \quad (2)$$

All experiments were performed in triplicate and the data are presented as mean ± standard error of mean. Summary of IC_{50} values (Table 1) shows that all seven kallikreins tested were inhibited by fukugetin to a greater or lesser degree. KLK2 and KLK1 showed the lowest values of IC_{50}, 3.2 μM and 5.7 μM, respectively. To better understand the interaction between KLK1 and KLK2 with fukugetin, we performed a detailed kinetic study to determine the mechanism of inhibition. Lineweaver–Burk or double-reciprocal plots, $1/v$ versus $1/[I]$, for KLK1 and KLK2, are show in Figure 1. This type of plot is especially useful for distinguishing between competitive and noncompetitive inhibition and in the calculations of the kinetic parameters.[21] The lines converge above the x axis to the same point in the second quadrant, for both enzymes, suggesting

Table 1
Inhibition of kallikreins by fukugetin

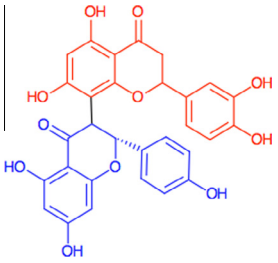

KLK	IC_{50} (μM)
KLK1	5.7 ± 0.2
KLK2	3.2 ± 0.1
KLK3	13 ± 0.8
KLK5	12.5 ± 1.1
KLK6	13.5 ± 0.3
KLK7	15 ± 0.5

IC_{50} values were determined from plots of percent inhibition versus log inhibitor concentration, and calculated by nonlinear regression. Molecular structure of Fukugetin is indicated in red (Luteolin domain) and blue color (Nareingenin domain blue).

that fukugetin acts as a mixed-type inhibitor for both enzymes, called linear partial competitive inhibition.[21] In addition we also plotted the Eadie–Hofstee graph (Fig. S1) that confirmed the mixed-type inhibition.

This type of inhibition occurs when the inhibitor binds to both E and ES, but its affinity for these two forms of the enzyme are different ($K_i \neq \alpha K_i$) and ESI complex is nonproductive (Fig. 1c). K_m and V_{max} were determined at each fukugetin concentration, and the data are show in Table 2. Mixed-type inhibitor affects the parameters K_m (increase) and V_{max} (decrease), interfering with catalysis and substrate binding.[21] To KLK1, K_m ranged between 0.65 ± 0.03 and 1.12 ± 0.1 μM; and V_{max} ranged between 450 ± 20 and 160 ± 12 μM·s^{-1}. In the case of KLK2, K_m ranged between 0.62 ± 0.02 and 1.20 ± 0.01 μM; and V_{max} ranged between 226 ± 10 and 79 ± 2 μM·s^{-1}. The factor α (Table 2), the parameter by which K_S changes when fukugetin interacts with the enzyme, was 1.6 ± 0.1 to KLK1 and 2.3 ± 0.2 to KLK2; and the factor β, the parameter by which k_{cat} is altered when the inhibitor interacts the enzyme, was equal to zero to both proteases. Since β is equal to zero, the secondary plots, $1/V_{max}$ and the K_m/V_{max} on the fukugetin concentration, for both kallikreins are linear (Supplementary material, Fig. S2), confirming linear partial competitive inhibition.[21] The results of Table 2 also show that fukugetin binds KLK1 with a K_i of 3.6 μM ± 0.2 and binds KLK2 with 1.6 ± 0.1 μM.

In order to rationalize the observed mechanism of inhibition, we performed molecular docking combined with molecular dynamics simulations to identify the putative binding site of fukugetin bound to KLK1. Initially, AutoDock 4.2 was used to scan the entire protein surface (blind docking) to predict its binding mode. The resulting 300 conformations of the ligand were processed by the built-in clustering analysis, which showed that 79 of the docked conformations fall into three large clusters around the substrate pocket (Fig. 2a). The first pocket has 35 conformations coming from only one cluster (C1) while the second pocket contains 44 conformations and it is a combination of two clusters (C2 and C3), which differ only in the way the ligand binds. The mean binding energy for three clusters is −8.9 (C1), −8.5 (C2), and −6.5 kcal/mol (C3), respectively. Based on the calculated binding energy, it is possible to assume that the binding mode of fukugetin in C3 is less favorable. But, it is difficult to assess in which one of the other two cluster (C1 vs C2) the ligand has higher affinity, as both have

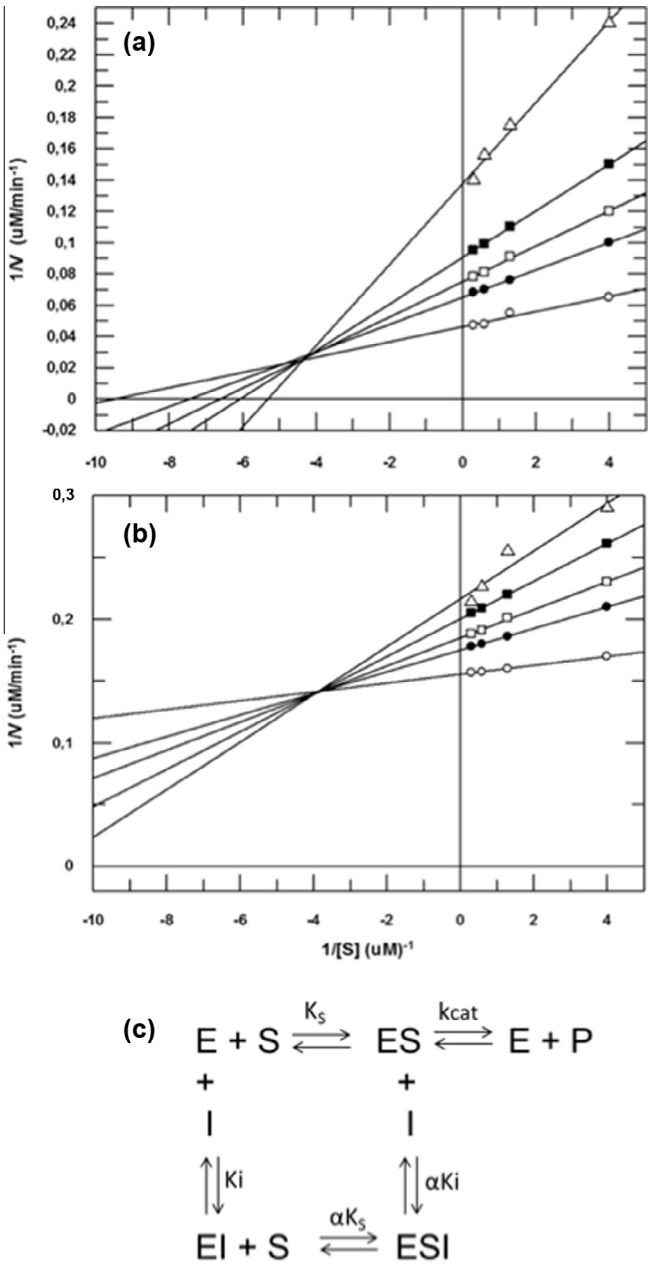

Figure 1. Lineweaver–Burk plot in absence (○) and in presence of different concentrations of fukugetin (● 2.0 μM, □ 4.0 μM, ■ 8.0 μM, △ 10.0 μM), for the hydrolysis of substrate Abz-KLRSSKQ-EDDnp by (a) KLK1 and (b) KLK2. (c) Schematic mechanism of inhibition for KLK1 and KLK2.

similar energies. So we decided to apply molecular dynamics simulations combined with Molecular Mechanics/Generalized Born Surface Area (MM/GBSA) as a more accurate method to investigate the KLK1-fukugetin binding. The lowest energy conformation from each of the three clusters was chosen as a representative (that we will call pose 1, 2 and 3 from now on) and was used as starting structures for 20 ns of MD simulations using Amber.

Pose 1 had a similar conformation to the starting one until 4 ns of the MD, when it underwent some conformational change, and the new conformation remained nearly constant for the rest of the trajectory, around 2.5 and 3.0 Å (Support information, Fig. S1). In this pose, the naringenin halve of fukugetin is located at the S1 pocket (Asp189, Thr190) and the other halve occupies the S2 pocket (Tyr99, His57, Trp215). The complex is stabilized by hydrophobic interactions with the amino acids of the S2 pocket and a π–π interaction with Tyr99 (Fig. 2b). Unlike pose 1, at the beginning of the simulation the conformation of pose 2 was significantly altered compared to the docked one, mainly at the luteolin halve, due the rotation around the C3–C8″ bond and the new conformation remained constant around 3.5 Å during the rest of simulation (Supplementary material, Fig. S3). This pose is stabilized by hydrophobic interactions with the amino acids of the S1′ and S2′ pocket (Gln41, Phe40, Phe151). Two hydrogens bond with of Gln41, and a π–π interaction with Phe151 further stabilize the complex (Fig. 2c). Finally, for pose 3 significant differences in its position and conformation were observed throughout the MD simulation. This pose gradually left the starting conformation and moves away from the binding pocket, losing its contact with the enzyme.

MM/PB(GB)SA was used to estimate relative free energy of binding (ΔG_{bind}) of the three poses based on 1500 snapshots extracted from the MD trajectories between 5 and 20 ns at a time interval of 2 ps. The calculated ΔG_{bind} using MM/GBSA for pose 1, 2 and 3 is −26.0, −25.4, and −10.4 kcal/mol, respectively. While, using the MM/PBSA approach the ΔG_{bind} values are 16.8, −0.5, and 6.1, respectively. Consistently with the trajectory analysis, the weakest binder, pose 3, can be distinguished from the other inhibitors, although less so with MM–PBSA than MM–GBSA. As for the other poses, the MM/GBSA method provides similar values for the ΔG_{bind} while MM/PBSA favors pose 2 over pose 1. These results are in agreement with the mechanism of inhibition of fukugetin and indicate that pose 2 is likely the one observed when the enzyme is free. At this stage, we cannot exclude that the inhibitor may also binds at an allosteric site in enzyme–substrate complex. In conclusion, here we describe an inhibitor with the capacity to interact with KLK1 and KLK2 in a mixed-type inhibitory mechanism. Our findings provide additional insight into the possible binding mode of fukugetin, and might have implications for further optimization of this inhibitor.

Table 2
Kinetic parameters from KLK1 and KLK2 inhibition by fukugetin (means ± standard deviation)

Fukugetin (μM)	0	2.0	4.0	8.0	10.0
		KLK1			
V_{max} (μM·s^{-1})	450 ± 20	387 ± 17	285 ± 15	201 ± 10	160 ± 12
K_m (μM)	0.65 ± 0.03	0.80 ± 0.04	0.85 ± 0.03	0.93 ± 0.06	1.12 ± 0.01
α	1.6 ± 0.1				
β	0				
K_i (μM)	3.6 ± 0.2				
		KLK2			
V_{max} (μM·s^{-1})	226 ± 10	192 ± 5	144 ± 3	110 ± 3	79 ± 2
K_m (μM)	0.62 ± 0.02	0.72 ± 0.02	0.81 ± 0.01	1.04 ± 0.01	1.20 ± 0.02
α	2.3 ± 0.2				
β	0				
K_i (μM)	1.6 ± 0.1				

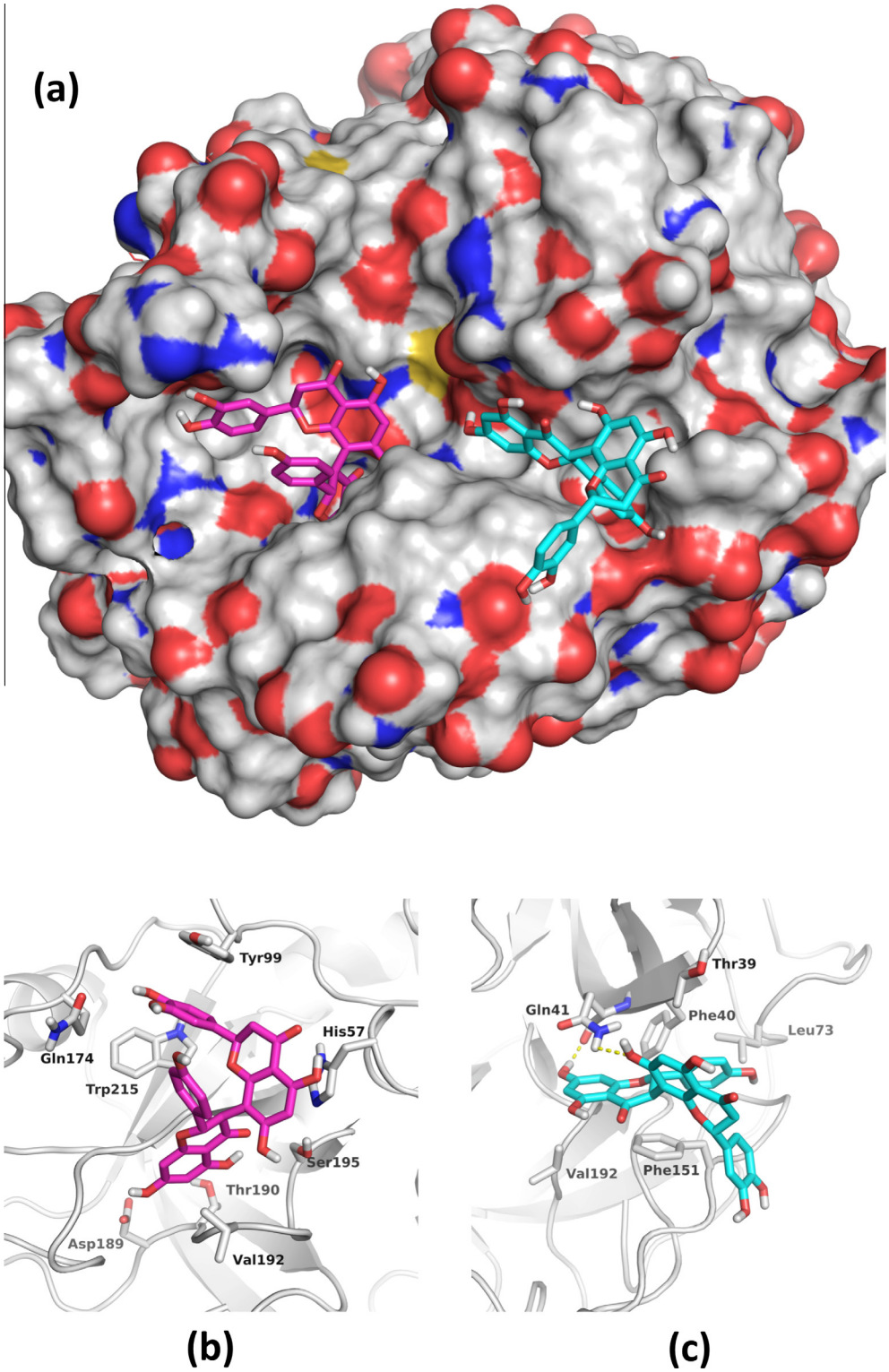

Figure 2. (a) Blind docking of fukugetin into the KLK1 identified two potential binding sites: Pose 1 (magenta) and pose 2 (cyan) are the lowest energy conformation from each of the two clusters. The surface of the enzyme is colored by atom type; (b) the MD-refined binding mode of pose 1; (c) the MD-refined binding mode of pose 2. Residues in the protein-binding pocket involved in specific interactions with fukugetin and hydrogen bonds (yellow dash line) are annotated.

Acknowledgement

We gratefully acknowledge financial support from FAPESP (Fundação de Amparo à Pesquisa do Estado de São Paulo, Proc. 2013/10548-3).

Supplementary data

Supplementary data associated with this article can be found, in the online version, at http://dx.doi.org/10.1016/j.bmcl.2016.01.039.

References and notes

1. Kontos, C. K.; Mavridis, K.; Talieri, M.; Scorilas, A. *Thromb. Haemost.* **2013**, *110*, 2013.
2. Li, H. X.; Hwang, B. Y.; Laxmikanthan, G.; Blaber, S. I.; Blaber, M.; Golubkov, P. A.; Ren, P.; Iverson, B. L.; Georgiou, G. *Protein Sci.* **2008**, *17*, 2008.
3. Clements, J. A.; Willemsen, N. M.; Myers, S. A.; Dong, Y. *Crit. Rev. Clin. Lab. Sci.* **2004**, *41*, 2004.
4. Pathak, M.; Wong, S. S.; Dreveny, I.; Emsley, J. *Thromb. Haemost.* **2013**, *110*, 2013.
5. Shaw, J. L.; Diamandis, E. P. *Clin. Chem.* **2007**, *53*, 2007.
6. Avgeris, M.; Mavridis, K.; Scorilas, A. *Biol. Chem.* **2012**, *393*, 2012.
7. Bhoola, K. D.; Figueroa, C. D.; Worthy, K. *Pharmacol. Rev.* **1992**, *44*, 1992.
8. Borgono, C. A.; Diamandis, E. P. *Cancer* **2004**, *4*, 2004.
9. Borgono, C. A.; Michael, I. P.; Shaw, J. L.; Luo, L. Y.; Ghosh, M. C.; Soosaipillai, A.; Grass, L.; Katsaros, D.; Diamandis, E. P. *J. Biol. Chem.* **2007**, *282*, 2007.
10. Pampalakis, G.; Scorilas, A.; Sotiropoulou, G. *Clin. Biochem.* **2008**, *41*, 2008.
11. Suzuki, J.; Yoshida, S.; Chen, Z. L.; Momota, Y.; Kato, K.; Hirata, A.; Shiosaka, S. *Neurosci. Res.* **1995**, *23*, 1995.
12. Gao, L.; Smith, R. S.; Chen, L. M.; Chai, K. X.; Chao, L.; Chao, J. *Biol. Chem.* **2010**, *391*, 2010.
13. Little, S. P.; Dixon, E. P.; Norris, F.; Buckley, W.; Becker, G. W.; Johnson, M.; Dobbins, J. R.; Wyrick, T.; Miller, J. R.; MacKellar, W.; Hepburn, D.; Corvalan, J.; McClure, D.; Liu, X.; Stephenson, D.; Clemens, J.; Johnstone, E. M. *J. Biol. Chem.* **1997**, *272*, 1997.
14. Stephan, C.; Jung, K.; Lein, M.; Diamandis, E. P. *Eur. J. Cancer* **2007**, *43*, 2007.
15. Angelo, P. F.; Lima, A. R.; Alves, F. M.; Blaber, S. I.; Scarisbrick, I. A.; Blaber, M.; Juliano, L.; Juliano, M. A. *J. Biol. Chem.* **2006**, *281*, 2006.
16. Freitas, R. F.; Teixeira, T. S.; Barros, T. G.; Santos, J. A.; Kondo, M. Y.; Juliano, M. A.; Juliano, L.; Blaber, M.; Antunes, O. A.; Abrahao, O., Jr.; Pinheiro, S.; Muri, E. M.; Puzer, L. *Bioorg. Med. Chem. Let.* **2012**, *22*, 2012.
17. Oliveira, J. P.; Freitas, R. F.; Melo, L. S.; Barros, T. G.; Santos, J. A.; Juliano, M. A.; Pinheiro, S.; Blaber, M.; Juliano, L.; Muri, E. M.; Puzer, L. *ACS Med. Chem. Let.* **2014**, *5*, 2014.
18. Teixeira, T. S.; Freitas, R. F.; Abrahao, O., Jr.; Devienne, K. F.; de Souza, L. R.; Blaber, S. I.; Blaber, M.; Kondo, M. Y.; Juliano, M. A.; Juliano, L.; Puzer, L. *Bioorg. Med. Chem. Let.* **2011**, *21*, 2011.
19. Assis, D. M.; Gontijo, V. S.; de Oliveira Pereira, I.; Santos, J. A.; Camps, I.; Nagem, T. J.; Ellena, J.; Izidoro, M. A.; dos Santos Tersariol, I. L.; de Barros, N. M.; Doriguetto, A. C.; dos Santos, M. H.; Juliano, M. A. *J. Enzyme Inhib. Med. Chem.* **2013**, *28*, 2013.
20. Bradford, M. M. *Anal. Biochem.* **1976**, *72*, 1976.
21. Segel, I. H. *Enzyme Kinetics Behavior and Analysis of Rapid Equilibrium and Steady-State Enzyme Systems*; John Wiley & Sons: New York, 1993. pp 470–473.